PHYSICAL REVIEW B **88**, 140301(R) (2013)

Terahertz macrospin dynamics in insulating ferrimagnets

Mostafa Shalaby,[1,*] Francois Vidal,[1] Marco Peccianti,[1,2] Roberto Morandotti,[1] Florian Enderli,[3] Thomas Feurer,[3] and Bruce D. Patterson[4,†]

[1]*Institut National de la Recherche Scientifique (INRS-EMT), Varennes, Quebec J3X 1S2, Canada*

[2]*Also at: Dept. of Physics and Astronomy, University of Sussex, Falmer, Brighton BN1 9QH, United Kingdom*

[3]*Institute of Applied Physics, University of Bern, Sidlerstrasse 5, CH-3012 Bern, Switzerland*

[4]*SwissFEL, Paul Scherrer Institut, CH-5232 Villigen PSI, Switzerland*

(Received 8 April 2013; revised manuscript received 10 September 2013; published 21 October 2013)

We investigate numerically the excitation of nonlinear magnetic interactions in a ferrite material by an energetic pump pulse of terahertz (THz) radiation. The calculations are performed by solving the coupled Maxwell and Landau-Lifshitz-Gilbert differential equations. In a time-resolved THz pump/THz probe scheme, it is demonstrated that Faraday rotation of a delayed THz probe pulse can be used to map these interactions. Our study is motivated by the ability of soft x-ray free electron lasers to perform time-resolved imaging of the magnetization process at the submicrometer and subpicosecond length and time scales.

DOI: 10.1103/PhysRevB.88.140301 PACS number(s): 75.78.−n, 33.57.+c, 78.20.Ls, 87.50.U−

Current research in ultrafast magnetization dynamics is being driven by applications in magnetic storage technology[1] and logic operations using spintronic devices.[2] For example, fundamental limits to the switching speed of a magnetic storage medium have been established, using the electron pulses from an electron accelerator to generate intense switching fields of ps duration,[3,4] and the generation, with optical laser pulses, of spin-polarized photocurrents in semiconductor quantum wells has been demonstrated.[5] At the same time, a powerful new tool for investigating (probing) magnetic phenomena at the nanometer and picosecond scales, the x-ray free electron laser (XFEL), is now becoming available.[6–9]

Although ultrafast demagnetization[10] and optomagnetic reorientation[11,12] can be initiated by intense optical laser pulses, the underlying effects are as yet poorly understood. A popular pump source for x-ray-based studies of dynamic magnetism is the pulsed current in a laser-switched strip line,[13,14] but the resulting magnetic field pulses are generally of low amplitude (0.01 T) and have a slow rise time (100 ps). Much progress is being made in the generation and detection of energetic pulses of THz radiation,[15–18] and there is much interest in the noninear interactions which such pulses may initiate.[19–22] Applied to magnetism, THz pulses have been shown to excite resonant modes.[23–25] In our present work, we use numerical simulations to investigate the conditions under which THz pulses can coherently drive nonlinear magnetic interactions and magnetization (switching) reversal in a ferrite.[26] In a recent report, Vicario *et al.*[27] experimentally demonstrated that an intense THz pulse can initiate nonresonant precession in a thin cobalt film, resulting in a fractional change in the magnetization of 0.005. Although a delayed x-ray pulse may turn out to be the best suited probe of these dynamics, we extend our study to demonstrate that a suitable THz probe can also reveal the ultrafast magnetic state,[28–30] through time-resolved polarization rotation analysis.

As a sample, we choose strontium iron oxide ($SrFe_{12}O_{19}$), which we have recently used to realize a THz isolator.[30] This material, as is the case with many related ferrites, is promising for studies of THz magnetization dynamics, because it is an insulating ferrimagnet with low losses at THz frequencies.[30,31]

Our goal is to follow in time and space the interactions between a THz electromagnetic pulse and a magnetic sample; the Maxwell and the Landau-Lifshitz-Gilbert (LLG) equations govern their behavior, respectively. Our approach to investigate the magnetic part of the problem is similar to the study of precessional magnetization dynamics under intense few-picoseconds-long magnetic field pulses.[3] The evolution of the magnetization $\boldsymbol{M}$ is determined by the instantaneous magnitude and direction of the local magnetic field, both of which vary with time and position as the pulse propagates. The relevant time and length scales are picoseconds and micrometers; the speed of THz propagation in our ferrite material is approximately 50 μm/ps.

We use a model which couples the LLG and Maxwell equations to perform the numerical simulation of a time-resolved THz pump/THz probe scheme. The LLG-based description of the time evolution of the magnetization $\boldsymbol{M}$ in the local magnetic field $\boldsymbol{H}_{\text{eff}}$ is[32]

$$\frac{\partial \boldsymbol{M}}{\partial t} = -|\gamma|\boldsymbol{M} \times \boldsymbol{H}_{\text{eff}} + \frac{\alpha}{M_s}\left(\boldsymbol{M} \times \frac{\partial \boldsymbol{M}}{\partial t}\right), \qquad (1)$$

where $\gamma = 22$ km A^{-1} s^{-1} is the gyromagnetic ratio. M_s and α are the material-dependent saturation magnetization and Gilbert damping coefficient, respectively. $\boldsymbol{H}_{\text{eff}}$ is the effective field acting on the magnetic moments and can be written as the sum of the contributions

$$\boldsymbol{H}_{\text{eff}} = \boldsymbol{H} + \boldsymbol{H}_{\text{d}} + \boldsymbol{H}_{\text{an}} + \boldsymbol{H}_{\text{ex}}. \qquad (2)$$

$\boldsymbol{H}$ is the externally applied field, i.e., the THz magnetic field in this study. $\boldsymbol{H}_d$ is the demagnetization field, which can be represented in terms of a demagnetization tensor N as $\boldsymbol{H}_d = -N\boldsymbol{M}$. This field depends on the sample shape. In the present case of a thin disk, it acts to enforce an in-plane magnetization. $\boldsymbol{H}_{an}$ is the crystal anisotropy field, which in our case of a uniaxial material favors the alignment of $\boldsymbol{M}$ along a particular crystallographic axis; $H_{an} = 2k_{an}/\mu_0 M_s$,

where k_{an} and μ_0 are the anisotropy constant and free space permeability, respectively.[32] Finally, $\boldsymbol{H}_{ex}$ is the exchange field, which is parallel to $\boldsymbol{M}$ and hence tends to align neighboring magnetic spins to maintain a spatially uniform magnetization.

Our choice of an insulating uniaxial ferrimagnet avoids complications with eddy currents. We further assume that the action of $\boldsymbol{H}_{ex}$ is to guarantee that the sample is magnetized as a single domain ($M = M_s$). This avoids the complication of domain boundaries.[33] In our calculations, an index-matched nonmagnetic layer is placed below the ferrite layer to prevent outgoing reflections. We are assuming a homogeneous situation in the transverse dimensions. This is interpreted as a THz spot and sample size which are both much larger than the sample thickness. Therefore, in the solution of Maxwell equations, we consider variations only in the propagation direction. We use a one-dimensional finite-difference time domain (FDTD) scheme to couple the magnetic system (described by the LLG equation) to the propagation behavior (Maxwell equations) through the relation $\boldsymbol{H} = \boldsymbol{B}/\mu_0 - \boldsymbol{M}$, where $\boldsymbol{B}$ is the magnetic induction.[32] Our simulation parameters are taken from our recent characterization of the magnetic medium and THz dielectric response of $SrFe_{12}O_{19}$ as part of a previous study.[30] We treat the sample as a lossy dielectric with the frequency-dependent dielectric function $\varepsilon = \varepsilon_\infty + \sigma/i\omega\varepsilon_0$ where ω and ε_0 are the angular frequency and free space permittivity, respectively.[34] We then have $\boldsymbol{D} = \varepsilon_0\varepsilon\boldsymbol{E}$ where $\boldsymbol{D}$ is the displacement vector and the remaining Maxwell curl equations are $\frac{\partial \boldsymbol{B}}{\partial t} = -\nabla \times \boldsymbol{E}$ and $\frac{\partial \boldsymbol{D}}{\partial t} = \nabla \times \boldsymbol{H}$. Our values for $\varepsilon_\infty = 36$ and the conductivity $\sigma = 40$ S m^{-1} were selected based on our THz time domain spectroscopy.[30] Our sample is assumed to be a 0.5-mm-thick disk placed in the x-z plane. The demagnetization field is along the sample normal (y direction) and so $\boldsymbol{H}_d = -M_y\hat{y}$. The z axis is taken to be the anisotropy axis. The magnetic material constants are taken to be $M_s = 360$ kA m^{-1}, as previously obtained from a vibrating sample magnetometer measurement,[30] $\alpha = 0.1$, and $k_{an} = 300$ kJ m^{-1}.

Figure 1(a) shows the pump and probe pulses for a specific pump-probe delay (τ_{pp}), defined as extending from the beginning of the pump pulse to the beginning of the probe pulse. As a pump, we choose an arbitrary single-cycle THz pulse (STP) with a central frequency of 0.22 THz. The probe is much shorter in duration and has a higher frequency, in order to increase the temporal resolution. The polarization configuration is shown in Fig. 1(b), with the THz electric and magnetic fields polarized along the z and x directions, respectively. $\boldsymbol{M}$ is initially aligned (as a single domain) along the z (crystal anisotropy) axis.

Since, as the LLG equation (1) indicates, the torque ($\boldsymbol{M} \times \boldsymbol{H}$) is the principal driving force for the magnetization dynamics, we maximize it by selecting an initial condition with $\boldsymbol{M} \perp \boldsymbol{H}$ [Fig. 1(b)]. This configuration is known as precessional switching and is distinguished from damping switching, for which $\boldsymbol{H}$ is initially set antiparallel to $\boldsymbol{M}$. For comparison, precessional switching allows for faster dynamics, but it requires a more intense field to accomplish switching.

In order to estimate the required THz field strength to produce magnetization dynamics in the THz regime, we solve

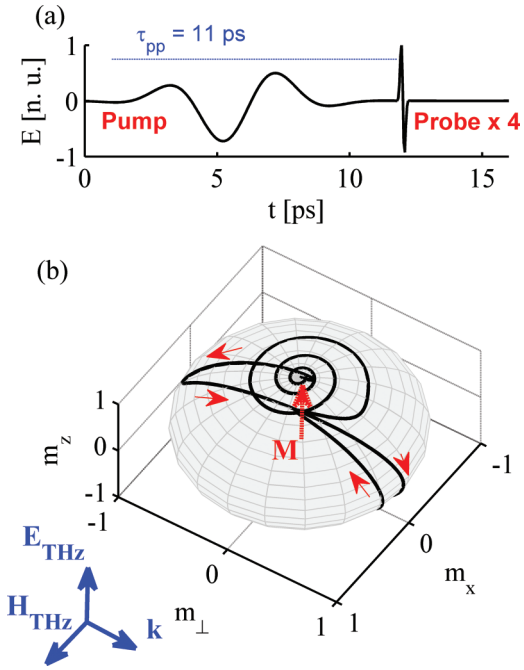

FIG. 1. (Color online) (a) The THz pump and probe pulses. (b) A schematic diagram showing the initial polarization convention. Both E_{THz} and H_{THz} lie in the plane of the sample surface. A unit sphere is shown to represent the magnetization state. A trajectory of the magnetization vector, after excitation by the THz pulse, is plotted on the sphere, with red arrows to indicate the time evolution.

the LLG equation of motion at $t = 0$, for the limiting case $\alpha = 0$. Note that this approach is similar to the Kittel model for ferromagnetic resonance,[35] but without a static magnetic field present. $\boldsymbol{H}_{\mathrm{eff}}$ can be expanded to

$$\boldsymbol{H}_{\mathrm{eff}} = \left(H^x + H^x_{ex}\right)\hat{x} + \left(H^y_d + H^y_{ex}\right)\hat{y} + \left(H^z_{an} + H^z_{ex}\right)\hat{z}. \quad (3)$$

$\boldsymbol{H}_{ex}$ is always parallel to $\boldsymbol{M}$ and hence plays no role here. At $t = 0$, $\boldsymbol{H}^y_d = 0$, and $\boldsymbol{H}_{an}$ has no influence, as it is initially parallel to $\boldsymbol{M}$. We assume a single frequency response for $\boldsymbol{M}$, and we calculate the instantaneous initial frequency to be $\omega = \gamma H_x$. After accounting for the reflections at the air-magnetic disk interface, we estimate that an incident THz peak field of 20 MV/cm (8.33 T) is sufficient to initiate magnetic interactions in the frequency regime 0.2–0.3 THz. The high refractive index of our sample leads to a significant reduction of the transmitted peak field to approximately 6 MV/cm (corresponding to an effective field amplitude and pulse duration of 4.2 MV/cm and 1.1 ps, respectively). A static field of this strength is comparable to the dc electric breakdown of insulators. However, the breakdown field strength increases significantly as the pulse duration decreases.[36,37] Therefore, we expect the dielectric breakdown to occur at much higher THz fields than those used in our calculations. Figure 1(b) shows a trajectory of the normalized magnetic vector ($m = m_x\hat{x} + m_y\hat{y} + m_z\hat{z}$ and $|m| = |M|/M_s = 1$) upon the application of the THz pump pulse. The initial torque ($\boldsymbol{M}_z \times \boldsymbol{H}_x$) builds up a significant out-of-plane magnetization $m_y = m_\perp$. This state is counteracted by a strong demagnetization, induced by the shape anisotropy. Following rapid dynamics occurring on the

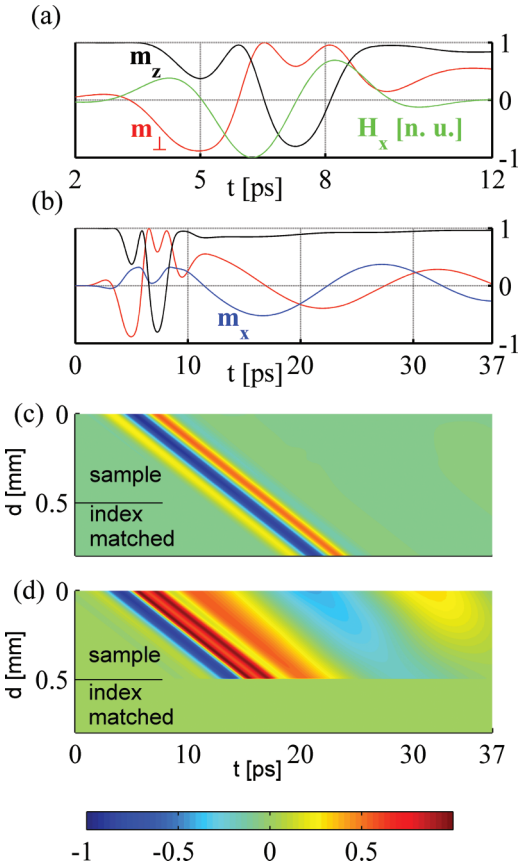

FIG. 2. (Color online) (a), (b) Time evolution of the THz field and magnetization components at a depth of 50 μm inside the sample. Space-time map of the THz pump magnetic field (c) and of the out-of-plane magnetization (d).

time scale of the THz pump pulse, $\boldsymbol{M}$ tends to damp into the sample plane, undergoing oscillations about and finally becoming aligned with the crystal anisotropy z axis. The components of magnetization dynamics are shown in Fig. 2. Initially, the THz-induced torque creates a strong out-of-plane component $m_\perp$ [Fig. 2(a)]. As $m_\perp$ grows, a torque component evolves in the z direction. With time, the changes in $m_\perp$ and m_z are counteracted by the demagnetization and anisotropy fields, respectively. These effects are strongest when the THz field reaches the zero-crossing point, favoring the equilibrium condition. As the THz pulse begins to grow again with opposite polarity, the 3D dynamics are again driven by the torque term. On the time scale of the THz pump pulse, the effect on m_x is weak. In our situation, this component is aligned with the THz magnetic field, and its influence on the dynamics is much less than that of the THz magnetic field. However, after the THz field is switched off, m_x becomes effective and replaces the THz in the dynamics. These delayed dynamics [Fig. 2(b)] are dominated by the damping term in the LLG equation and a relatively slow oscillation about the anisotropy z axis. The dynamics are shown in Figs. 2(a) and 2(b) at a specific depth inside the film. However, the field and magnetization components propagate through the sample with the velocity $\sim$50 μm/ps, as depicted in the space-time maps of Figs. 2(c) and 2(d). In our calculations we used a single-cycle terahertz pulse, which leads to a complete magnetization reversal (first half of the cycle) followed by its cancellation (second half of the cycle). A properly shaped Gaussian-like half-cycle terahertz pulse would avoid the cancellation and hence result in switching.

Ferrimagnets consist of multiple sublattices, and each sublattice should in principle be described by a separate LLG equation, coupled by interlattice exchange fields. Alternatively, unless the temperature is close to the ferrite compensation temperature,[38] it is possible to describe the entire ferrimagnetic system using a single LLG equation with effective values for the gyromagnetic ratio and the damping constant.[39,40] It is the latter approach that is used here. In a first approximation, the effective gyromagnetic ratio is set to the electron value $\gamma = 22$ km A^{-1} s^{-1} (with a g factor of 2) and the typical value $\alpha = 0.1$ is used as the effective damping constant. While these values are likely not exact at any temperature of the material considered, they are sufficiently accurate to illustrate the general trends, which is the main purpose of this Rapid Communication.

We have neglected phononic and ionization dynamics in our insulating sample. Acoustic phonons are expected to be only very weakly excited at 0.2 THz.[41] Optical phonon resonances occur at much higher frequencies (>12 THz[23]) than our THz pulse. Furthermore, because the THz photon energy is very small (0.2 THz corresponds to 0.834 meV), ionization can only result from massive multiple-photon absorption. This property is a particularly important reason to use nonionizing THz radiation in studies of magnetism dynamics. This is in contrast to the optical regime,[10] where the high energy of optical photons leads to electronic excitation and demagnetization.

We now pose the question: How can these magnetization dynamics, in particular the post-pump oscillations of m about the anisotropy field, be experimentally observed? In general, a modification of the transmitted pump pulse will contain information on the magnetization dynamics. It has been predicted that nonlinear magnetic interactions will modulate the wave form of a low-frequency electromagnetic pulse after propagation through a ferrimagnet.[42] At THz frequencies, however, the effective inertia of the magnetic system causes the changes in a transmitted pump pulse to be small. We therefore investigate the interaction of the pumped dynamic system with a delayed, high-frequency THz probe pulse.

Figure 3 depicts the effects of magnetization dynamics on a probe pulse with amplitude $\sim$1/3 that of the pump. We consider two pump-probe delays of 10 ps [Fig. 3(b)] and 20 ps [Fig. 3(c)], corresponding to a positive and a negative value of the oscillating $m_\perp$, respectively. [Note that for the slow, post-pump oscillations, $m_\perp$ is approximately constant over the sample thickness as seen in Fig. 2(d).] In both cases, a new component, E_x, of the transmitted pulse is observed, indicating a Faraday rotation of the probe polarization. The reversal of the sign of $m_\perp$ induces a π phase shift of E_x (that is a change of sign), due to a reversal of the sense of rotation of the polarization plane [see magnified E_x fields in Figs. 3(b) and 3(c)]. The rotation angle θ (calculated in the frequency domain at 2.5 THz) is computed for different delays [Fig. 3(d)] and compared with $m_\perp$ at a depth in the sample of 50 μm. Very good agreement between the two curves is obtained, demonstrating the effectiveness of Faraday rotation

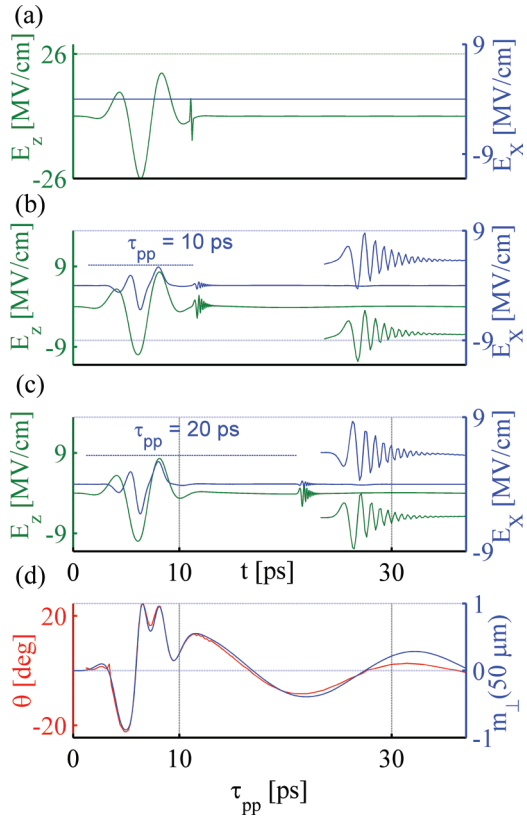

FIG. 3. (Color online) The input THz fields (a), and the transmitted THz fields at a pump-probe delay of (b) 10 ps and (c) 20 ps. The transmitted probe pulses are shown on a magnified scale at the right of the figure. (d) Faraday rotation of the transmitted THz probe pulse in comparison with $m_\perp$ at a depth of 50 μm.

in sensing the out-of-plane component of the magnetization. The maximum rotation found is 21.3°.

Finally, we compare the simulated rotation angle to the value predicted from standard theory.[31] At the THz frequencies, Faraday rotation in ferrites is approximately frequency independent. The rotation angle is given by $\theta = (l/2c)\sqrt{(|\varepsilon| + \varepsilon^1)/2}(M_s|\gamma|)$, where l, c, $|\varepsilon|$, and ε^1 are the sample thickness, the speed of light, the absolute value of the dielectric constant, and the real part of the dielectric constant, respectively.[31] In our case, $|\varepsilon| \approx \varepsilon^1 = 36$. For our material parameters, this suggests $\theta = 22.9°$ over 0.5 mm. This also agrees well with the result from our recent measurement of THz Faraday rotation in $SrFe_{12}O_{19}$:[30] a rotation of 105°/3 mm at 88% of saturation, which corresponds to 20° for our sample thickness. Here the calculation refers to a single frequency component. Shorter pulses, implying higher frequencies, are expected to give better temporal resolution but at the expense of higher attenuation, since losses increase with frequency, but the rotation is invariant. Frequency-independent Faraday rotation at THz frequencies arises from the fact that magnetic resonance in ferrites lies in the sub-THz regime. This leads to a rotation which is given by the frequency-independent formula given above. Although the dielectric constant can, in principle, induce a slight spectral dependence, this is negligible in our case of an insulating magnet.[30,31]

In conclusion, we have shown, by the numerical solution of coupled LLG and Maxwell equations, that an intense THz pulse can effectively trigger ultrafast magnetic switching and picosecond-scale magnetization dynamics. Our calculations also show that a delayed THz probe is capable of monitoring these dynamics through a magnetization-induced rotation of the polarization plane. Experiments are foreseen to demonstrate that THz pump–THz probe Faraday rotation is indeed feasible. With the advent from an XFEL of bright pulses of circularly polarized x rays which are resonant with $2p \rightarrow 3d$ absorption in transition-metal ions, it will be possible to directly monitor THz-induced magnetization dynamics in time and space.

M.S. and B.D.P. would like to gratefully thank G. L. Carr (BNL, NY) for suggesting the project[26] and L. J. Heyderman (ETH Zurich), M. Klaeui (EPF Lausanne), and R. Allensbach (IBM, Zurich) for their insights on micromagnetism. This work is supported by the Canadian FQRNT and NSERC, and the Swiss SNSF NCCR MUST funding agencies. M.S. and F.E. wish to acknowledge a FQRNT (MELS) scholarship and a SNSF 200020-119934 scholarship, respectively.

*shalaby@emt.inrs.ca

†bruce.patterson@psi.ch

[1] G. Hadjipanayis, *Magnetic Storage Systems Beyond 2000*, NATO Science Series, II: Mathematics, Physics, and Chemistry Vol. 41 (Kluwer Academic Publishers, Dordrecht, the Netherlands, 2001).

[2] S. Bader and S. Parkin, Annu. Rev. Condens. Matter Phys. **1**, 71 (2010).

[3] C. H. Back, R. Allenspach, W. Weber, S. S. P. Parkin, D. Weller, E. L. Garwin, and H. C. Siegmann, Science **285**, 864 (1999).

[4] I. Tudosa, C. Stamm, A. B. Kashuba, F. King, H. C. Siegmann, J. Stohr, G. Ju, B. Lu, and D. Weller, Nature (London) **428**, 831 (2004).

[5] S. D. Ganichev and W. Prettl, J. Phys.: Condens. Matter **15**, R935 (2003).

[6] C. Gutt, S. Streit-Nierobisch, L.-M. Stadler, B. Pfau, C. M. Günther, R. Könnecke, R. Frömter, A. Kobs, D. Stickler, H. P. Oepen *et al.*, Phys. Rev. B **81**, 100401 (2010).

[7] P. Emma, R. Akre, J. Arthur, R. Bionta, C. Bostedt, J. Bozek, A. Brachmann, P. Bucksbaum, R. Coffee, F.-J. Decker *et al.*, Nat. Photonics **4**, 641 (2010).

[8] B. D. Patterson, R. Abela, H.-H. Braun, U. Flechsig, R. Ganter, Y. Kim, E. Kirk, A. Oppelt, M. Pedrozzi, S. Reiche *et al.*, New J. Phys. **12**, 035012 (2010).

[9] S. Eisebitt, J. Luning, W. F. Schlotter, M. Lorgen, O. Hellwig, W. Eberhardt, and J. Stohr, Nature (London) **432**, 885 (2004).

[10] E. Beaurepaire, J.-C. Merle, A. Daunois, and J.-Y. Bigot, Phys. Rev. Lett. **76**, 4250 (1996).

[11] C. D. Stanciu, F. Hansteen, A. V. Kimel, A. Kirilyuk, A. Tsukamoto, A. Itoh, and T. Rasing, Phys. Rev. Lett. **99**, 047601 (2007).

[12]K. Vahaplar, A. M. Kalashnikova, A. V. Kimel, D. Hinzke, U. Nowak, R. Chantrell, A. Tsukamoto, A. Itoh, A. Kirilyuk, and T. Rasing, Phys. Rev. Lett. **103**, 117201 (2009).

[13]J. Raabe, C. Quitmann, C. H. Back, F. Nolting, S. Johnson, and C. Buehler, Phys. Rev. Lett. **94**, 217204 (2005).

[14]H. Stoll, A. Puzic, B. van Waeyenberge, P. Fischer, J. Raabe, M. Buess, T. Haug, R. Hollinger, C. Back, D. Weiss *et al.*, Appl. Phys. Lett. **84**, 3328 (2004).

[15]W. Shi, Y. J. Ding, N. Fernelius, and K. Vodopyanov, Opt. Lett. **27**, 1454 (2002).

[16]D. Daranciang, J. Goodfellow, M. Fuchs, H. Wen, S. Ghimire, D. A. Reis, H. Loos, A. S. Fisher, and A. M. Lindenberg, Appl. Phys. Lett. **99**, 141117 (2011).

[17]J. Dai, X. Xie, and X.-C. Zhang, Phys. Rev. Lett. **97**, 103903 (2006).

[18]C. Ruchert, C. Vicario, and C. P. Hauri, Opt. Lett. **37**, 899 (2012).

[19]T. Qi, Y.-H. Shin, K.-L. Yeh, K. A. Nelson, and A. M. Rappe, Phys. Rev. Lett. **102**, 247603 (2009).

[20]M. C. Hoffmann, N. C. Brandt, H. Y. Hwang, K.-L. Yeh, and K. A. Nelson, Appl. Phys. Lett. **95**, 231105 (2009).

[21]M. Liu, H. Y. Hwang, H. Tao, A. C. Strikwerda, K. Fan, G. R. Keiser, A. J. Sternbach, K. G. West, S. Kittiwatanakul, J. Lu *et al.*, Nature (London) **487**, 345 (2012).

[22]T. Koichiro, H. Hirori, and M. Nagai, Terahertz Science and Technology, IEEE Transactions on **1**, 301 (2011).

[23]T. Kampfrath, A. Sell, G. Klatt, A. Pashkin, S. Mahrlein, T. Dekorsy, M. Wolf, M. Fiebig, A. Leitenstorfer, and R. Huber, Nat. Photonics **5**, 31 (2011).

[24]A. Namai, M. Yoshikiyo, K. Yamada, S. Sakurai, T. Goto, T. Yoshida, T. Miyazaki, M. Nakajima, T. Suemoto, H. Tokoro *et al.*, Nat. Commun. **3**, 1035 (2012).

[25]K. Yamaguchi, M. Nakajima, and T. Suemoto, Phys. Rev. Lett. **105**, 237201 (2010).

[26]Private communication from G. L. Carr in 2009 suggesting performing single-pulse terahertz pump-probe spectroscopy of a magnetic sheet, as an extension of the low-frequency calculations of Ref. 42 to the terahertz regime (Brookhaven National Laboratory).

[27]C. Vicario, C. Ruchert, F. Aradana-Lamas, P. M. Derlet, B. Tudu, J. Luning, and C. P. Hauri, Nat Photonics **7**, 720 (2013).

[28]M. Shalaby, M. Peccianti, Y. Ozturk, M. Clerici, I. Al-Naib, L. Razzari, T. Ozaki, A. Mazhorova, M. Skorobogatiy, and R. Morandotti, Appl. Phys. Lett. **100**, 241107 (2012).

[29]A. M. Shuvaev, G. V. Astakhov, A. Pimenov, C. Brüne, H. Buhmann, and L. W. Molenkamp, Phys. Rev. Lett. **106**, 107404 (2011).

[30]M. Shalaby, M. Peccianti, Y. Ozturk, and R. Morandotti, Nat. Commun. **4**, 1558 (2013).

[31]C. L. Hogan, Rev. Mod. Phys. **25**, 253 (1953).

[32]J. M. D. Coey, *Magnetism and Magnetic Materials* (Cambridge University Press, Cambridge, England, 2010).

[33]C. Kittel, Phys. Rev. **71**, 270 (1947).

[34]D. Sullivan, *Electromagnetic Simulation Using the FDTD Method*, IEEE Press Series on RF and Microwave Technology (Wiley-IEEE, NJ, USA, 2000).

[35]C. Kittel, Phys. Rev. **73**, 155 (1948).

[36]D. Du, X. Liu, G. Korn, J. Squier, and G. Mourou, Appl. Phys. Lett. **64**, 3071 (1994).

[37]A.-C. Tien, S. Backus, H. Kapteyn, M. Murnane, and G. Mourou, Phys. Rev. Lett. **82**, 3883 (1999).

[38]S. Wienholdt, D. Hinzke, and U. Nowak, Phys. Rev. Lett. **108**, 247207 (2012).

[39]R. K. Wangsness, Phys. Rev. **91**, 1085 (1953).

[40]C. D. Stanciu, A. V. Kimel, F. Hansteen, A. Tsukamoto, A. Itoh, A. Kiriliyuk, and Th. Rasing, Phys. Rev. B **73**, 220402 (2006).

[41]T. E. Wilson, in *Proc. SPIE 6010, Infrared to Terahertz Technologies for Health and the Environment, Boston, MA* (SPIE, Bellingham, WA, 2005).

[42]R. Luebbers, K. Kumagai, S. Adachi, and T. Uno, Electromagnetic Compatibility, IEEE Transactions on **35**, 90 (1993).